

## THE VARIATION OF GALAXY MORPHOLOGICAL TYPE WITH ENVIRONMENTAL SHEAR

JOUNGHUN LEE AND BOMEEL LEE

Department of Physics and Astronomy, Frontier Physics Research Division, Seoul National University,  
Seoul 151-747, South Korea; jounghun@astro.snu.ac.kr, bmlee@astro.snu.ac.kr

Received 2008 January 9; accepted 2008 July 28

### ABSTRACT

Recent  $N$ -body simulations indicate that the assembly history of galactic halos depends on the density of the large-scale environment. This implies that galaxy properties such as age and size of the bulge may also vary with the surrounding large-scale structures, which are characterized by tidal shear as well as density. Using a sample of 15,882 well-resolved nearby galaxies from the Tully catalog and the real-space tidal field reconstructed from the 2MASS Redshift Survey, we investigate the dependence of galaxy morphological type on the shear of the large-scale environment in which they are embedded. We first calculate the large-scale dimensionless overdensities ( $\delta$ ) and ellipticities ( $e$ ) of the regions where the galaxies are located, classify them according to morphological type, and create subsamples selected at similar  $\delta$ -values but spanning different ranges in  $e$ . We calculate the mean ellipticity,  $\langle e \rangle$ , averaged over each subsample and find a signal of variation of  $\langle e \rangle$  with morphological type: for  $0.5 \leq \delta \leq 1.0$ , elliptical galaxies are preferentially located in regions with low ellipticity; for  $-0.3 \leq \delta \leq 0.1$ , the latest-type spirals are preferentially located in regions with high ellipticity. The null hypothesis that the mean ellipticities of the regions where the ellipticals and the latest-type spirals are located are the same as the global mean ellipticity averaged over all types is rejected at the  $3\sigma$  level when  $-0.3 \leq \delta \leq 0.1$ . Yet, no signal of a galaxy-shear correlation is found in highly overdense or underdense regions. The observed trend suggests that the formation epochs of galactic halos might be a function of not only halo mass and large-scale density but also large-scale shear. Since the statistical significance of the overall trend is low, a sample of at least 100,000 galaxies is required to verify this correlation.

*Subject headings:* cosmology: observations — large-scale structure of universe

### 1. INTRODUCTION

It has long been known that the physical properties of galaxies, such as morphological type, color, luminosity, spin parameter, star formation rate, concentration parameter, and so on, are functions of environment (Dressler 1980; Postman & Geller 1984; Whitmore et al. 1993; Lewis et al. 2002; Gómez et al. 2003; Goto et al. 2003; Rojas et al. 2005; Kuehn & Ryden 2005; Blanton et al. 2005; Bernardi et al. 2006; Choi et al. 2007; Park et al. 2007). Most previous work has focused on galaxies located in highly dense regions and usually quantified the environmental dependence of galaxy properties in terms of cross-correlations with the local density on small scales, which are believed to be established by environmentally dependent processes such as galaxy-galaxy interactions.

The currently popular  $\Lambda$ CDM model predicts that galaxy properties are correlated with not only the small-scale but also the large-scale environment. Here the “small” and “large” scales represent surrounding regions smaller and larger than  $5 h^{-1}$  Mpc, respectively. Recent high-resolution  $N$ -body simulations of a  $\Lambda$ CDM cosmology have demonstrated that the assembly history of galactic halos of a given mass changes with the density field if smoothed on sufficiently large scales (Gao et al. 2005). Since a galaxy’s content depends strongly on the assembly history of its host halo (Springel et al. 2005; Croton et al. 2007), this numerical finding suggests that the intrinsic properties of galaxies may be correlated with the density of the large-scale environment.

In fact, several groups have already found observational evidence for the existence of cross-correlations between galaxy properties and large-scale tidal shear. Navarro et al. (2004) found that the spin axes of spiral galaxies near the Local Supercluster lie preferentially on the supergalactic plane. Trujillo et al. (2006)

also showed by analyzing recent observational data from large galaxy surveys that the spin axes of void galaxies tend to be inclined to the void surfaces, retaining an initial memory of tidally induced alignment. Pandey & Bharadwaj (2006) have shown that galaxy luminosity and color depend on the filamentarity of the large-scale environment. More recently, they also presented the result that the star formation rates of galaxies are correlated with the filamentarity of the surrounding large-scale structure (Pandey & Bharadwaj 2008). Hernandez et al. (2007) found a one-to-one correspondence between the value of the galaxy spin parameter and morphological type, while Hernandez & Cervantes-Sodi (2006) and Cervantes-Sodi & Hernandez (2008) have noted that the spin parameters of observed galaxies are strongly correlated with their color and chemical abundance.

The existence of cross-correlations between galaxy properties and the density of the large-scale environment implies that the galaxies’ content still has a memory of the initial conditions of the Lagrangian regions where the host halos formed. In the scenario of biased formation, galaxy sites correspond to high peaks in the linear density field (Kaiser 1984; Bardeen et al. 1986). But since the initial density peaks are not spherical, they should be characterized not only by peak height but also by ellipticity and prolateness. Hence, if galaxy properties are still linked to the large-scale density, it is likely that they are also linked to the large-scale ellipticity and prolateness.

Our goal here is to test this statistical link. Instead of the ellipticity of the large-scale density field, however, we consider the ellipticity of the large-scale potential field (i.e., the tidal shear). Since the potential field is smoother than the density field, we believe that the large-scale potential field more directly reflects the linear conditions. Furthermore, the tidal shear field, defined as the second derivative of the potential field, has a large-scale

TABLE 1  
GALAXY SAMPLES

Sample	Class	Type	$N_g$
E.....	Elliptical	cE, E0, E0-1, E+	1008
L.....	Lenticular	S0 <sup>-</sup> , S0 <sup>0</sup> , S0 <sup>+</sup>	2532
SI.....	Spiral	S0a, Sa	1761
SII.....	Spiral	Sab, Sb	3175
SIII.....	Spiral	Sbc, Sc	4507
SIV.....	Spiral	Scd, Sd, Sdm, Sm	2679

coherence, resulting in a highly anisotropic spatial distribution of galaxies at the present epoch (Bond et al. 1996). Therefore, the tidal shear field is more readily measurable from the large-scale spatial distribution of present-day galaxies.

In previous approaches, however, the correlation between galaxy properties and the large-scale shear was measured in redshift space. Since redshift distortion could contaminate measurements of the filamentarity of the large-scale structure, it is desirable to measure this property in real space. Moreover, true as it is that in the linear regime the density and tidal shear in a given region are mutually independent, it is likely that the two quantities have developed cross-correlations in the subsequent nonlinear regime. Therefore, to find an independent relationship between galaxy properties and large-scale tidal shear, one has to first account for the density-shear correlations and remove their effect.

We attempt here to measure observationally an independent relationship between the morphological types of nearby large galaxies and the real-space tidal shear reconstructed from an all-sky survey. The organization of this paper is as follows: In § 2, the observational data are described. In § 3, the environmental shear is defined and its mean value, averaged over a number of galaxy subsamples at similar density, is measured as a function of galaxy morphological type. In § 4, the results are discussed and final conclusions are drawn.

## 2. OBSERVATIONAL DATA: AN OVERVIEW

A total of 35,000 galaxies with spectroscopic information are listed in the Tully catalog (B. Tully, private communication), which was constructed from the ESO/Uppsala full-sky survey (Nilson 1973; Lauberts 1982). Only 15,922 galaxies in the Tully catalog have detailed information on morphological type, determined by B. Tully according to the conventional Hubble classification scheme. For a detailed description of the Hubble scheme, see Table 2 in the Third Reference Catalogue of Bright Galaxies (RC3; de Vaucouleurs et al. 1991). For the remaining 19,078 galaxies in the Tully catalog, the morphological types are described as either “irregular” or “uncertain” or “doubtful” or “spindle,” “outer ring,” or “pseudo-outer R.” These are excluded from our analysis.

According to the morphological type described in the RC3, we divide the selected Tully galaxies into six samples: E, L, SI, SII, SIII, and SIV. Table 1 lists the class, the morphological type (as in the RC3), and the number of galaxies ( $N_g$ ) for each: sample E contains only elliptical galaxies, with Hubble types of cE, E0, E0-1, and E+; sample L contains only lenticular galaxies with the Hubble types of S0<sup>-</sup>, S0<sup>0</sup>, and S0<sup>+</sup>; sample SI consists of spirals of types S0/a and Sa, which have tightly wound arms and the largest bulges. The spirals of type Scd, Sd, Sdm, and Sm belong to sample SIV; these have no well-developed bulge and loosely wound arms. Sample SII contains the spirals of type Sa as well as type Sab, which are intermediate between Sa and Sb. Likewise, sample SIII contains the spirals of type Sb and Sbc. As

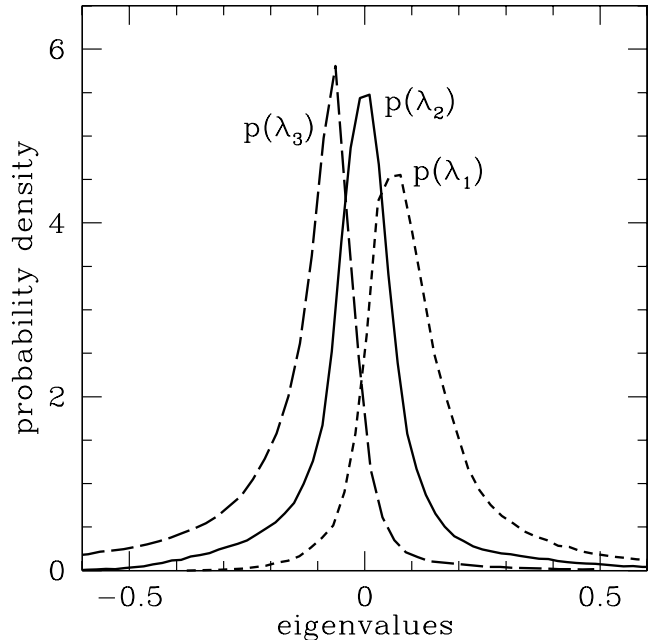


FIG. 1.—Probability density distributions of the three eigenvalues of the 2MRS tidal shear field.

can be noted, the size of the bulge and the tightness of the spiral arms decrease from SI to SIV.

The real-space density field was originally reconstructed on a  $64^3$  grid in a box of linear size  $400 h^{-1}$  Mpc from the 2MASS Redshift Survey (2MRS; Erdoğdu et al. 2006). Basically, it is the linear density field smoothed with a Wiener filter assuming a linear bias. Lee & Erdoğdu (2007) used the 2MRS density field to reconstruct the tidal shear field on the same  $64^3$  grid. As described in detail by Erdoğdu et al. (2006), the real-space positions were recovered by applying the Wiener reconstruction algorithm to the 2MRS data. This algorithm basically deconvolves the linear redshift distortions in the radial direction using a distortion matrix. For a detailed description of the method used to recover the real-space position, see Erdoğdu et al. (2006).

The reconstructed tidal shear field consists of a set of three eigenvalues,  $\{\lambda_1, \lambda_2, \lambda_3\}$ , of the tidal shear tensor assigned to each grid point. Figure 1 plots the probability density distributions of the three eigenvalues of the 2MRS tidal field, assuming  $\lambda_1 \geq \lambda_2 \geq \lambda_3$ . As can be seen, the distribution of the second-largest eigenvalue,  $p(\lambda_2)$ , is almost symmetric around the peak at zero with narrow width, while the other two distributions  $p(\lambda_1)$  and  $p(\lambda_3)$  are asymmetric around zero with broader shapes.

The differences among the eigenvalues are related to the shear of the environment at a given grid point. If  $\lambda_1 = \lambda_2 = \lambda_3$ , the shear of the environment is zero. The larger the mutual differences among the eigenvalues are, the higher the shear of the environment is. Figure 2 plots the 2MRS tidal shear eigenvalue field evaluated on a thin shell at  $80 h^{-1}$  Mpc, shown in supergalactic Aitoff projection. The top, middle, and bottom panels show the  $\lambda_1$ ,  $\lambda_2$ , and  $\lambda_3$  fields, respectively. In each panel, the darker regions correspond to low eigenvalues, while the bright regions correspond to high eigenvalues.

By applying the cloud-in-cell interpolation method (Hockney & Eastwood 1988) to the 2MRS tidal shear field, Lee & Erdoğdu (2007) also calculated the tidal tensors and their eigenvalues at the positions of the 15,922 selected Tully galaxies. Using the reconstructed 2MRS tidal shear field, we measure the values of the shear at the positions of the Tully galaxies. In the next section,

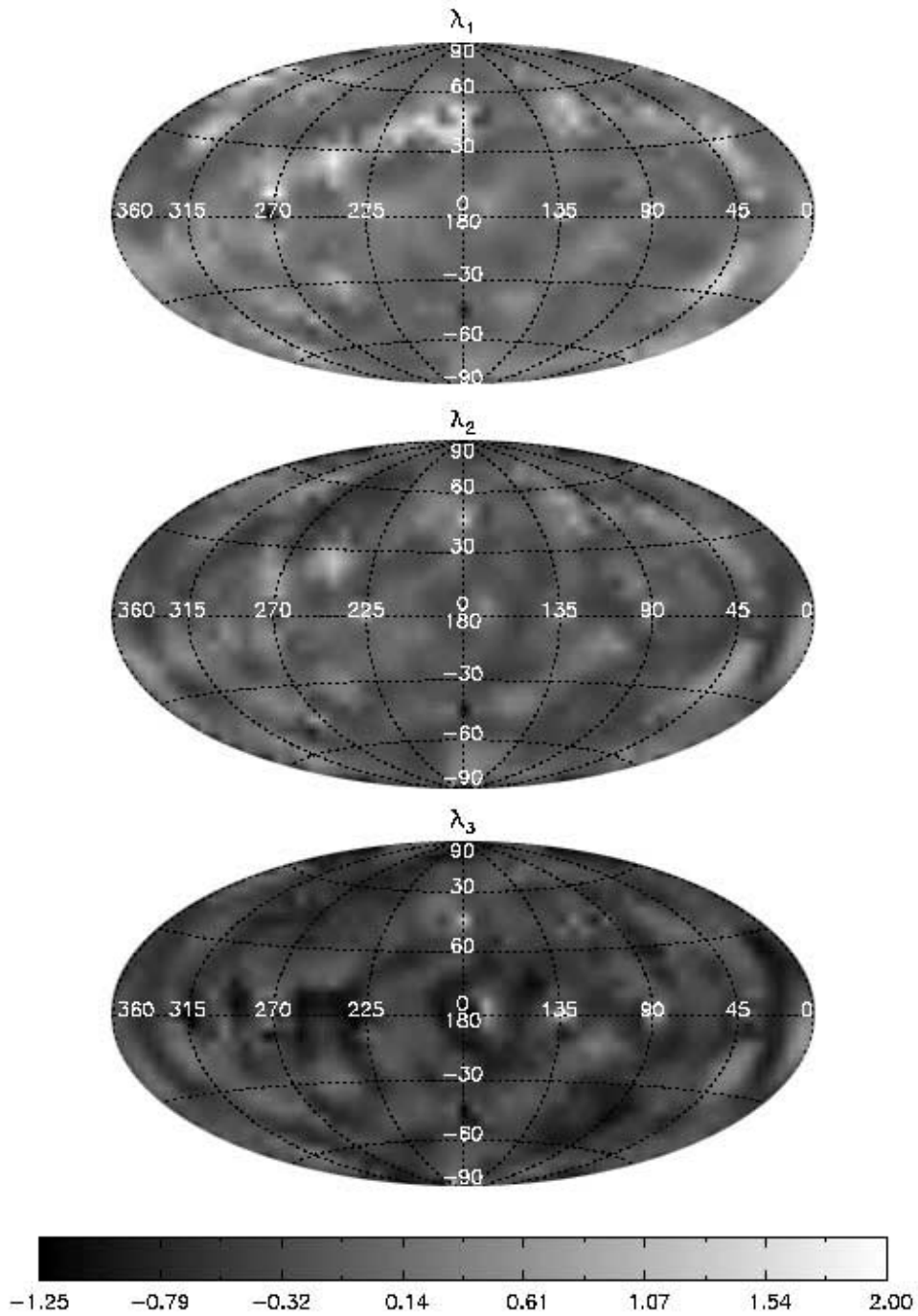


FIG. 2.—Aitoff projections of the tidal shear eigenvalue field in supergalactic coordinates at  $8000 \text{ km s}^{-1}$ :  $\lambda_1$  (top),  $\lambda_2$  (middle),  $\lambda_3$  (bottom).

we show how these measured shears are related to the morphological types of the Tully galaxies.

### 3. GALAXY-SHEAR CORRELATIONS

#### 3.1. Variation with Large-Scale Structure

Let us consider a position,  $\mathbf{x}$ , where a selected Tully galaxy is located. Whether the galaxy belongs to a void or a sheet or a filament or a halo depends on the signs of  $\lambda_1$ ,  $\lambda_2$ , and  $\lambda_3$  at  $\mathbf{x}$ . If all three eigenvalues are positive at  $\mathbf{x}$ , then the galaxy is located in a

halo-like region; if  $\lambda_2 > 0$  and  $\lambda_3 < 0$ , then it is in a filament-like region; if  $\lambda_1 > 0$  and  $\lambda_2 < 0$ , then it is in a sheetlike region; if  $\lambda_1 < 0$ , it is in a voidlike region.

We investigate the dependence of the relative abundance of the sample galaxies located in halo-like regions on morphological type by measuring the conditional number density (CND):

$$\frac{\delta N_{\text{type}}}{\delta N_{\text{all}}} \equiv \frac{\Delta N_{\text{type}}}{N_{\text{type}}} \frac{N_{\text{all}}}{\Delta N_{\text{all}}}. \quad (1)$$

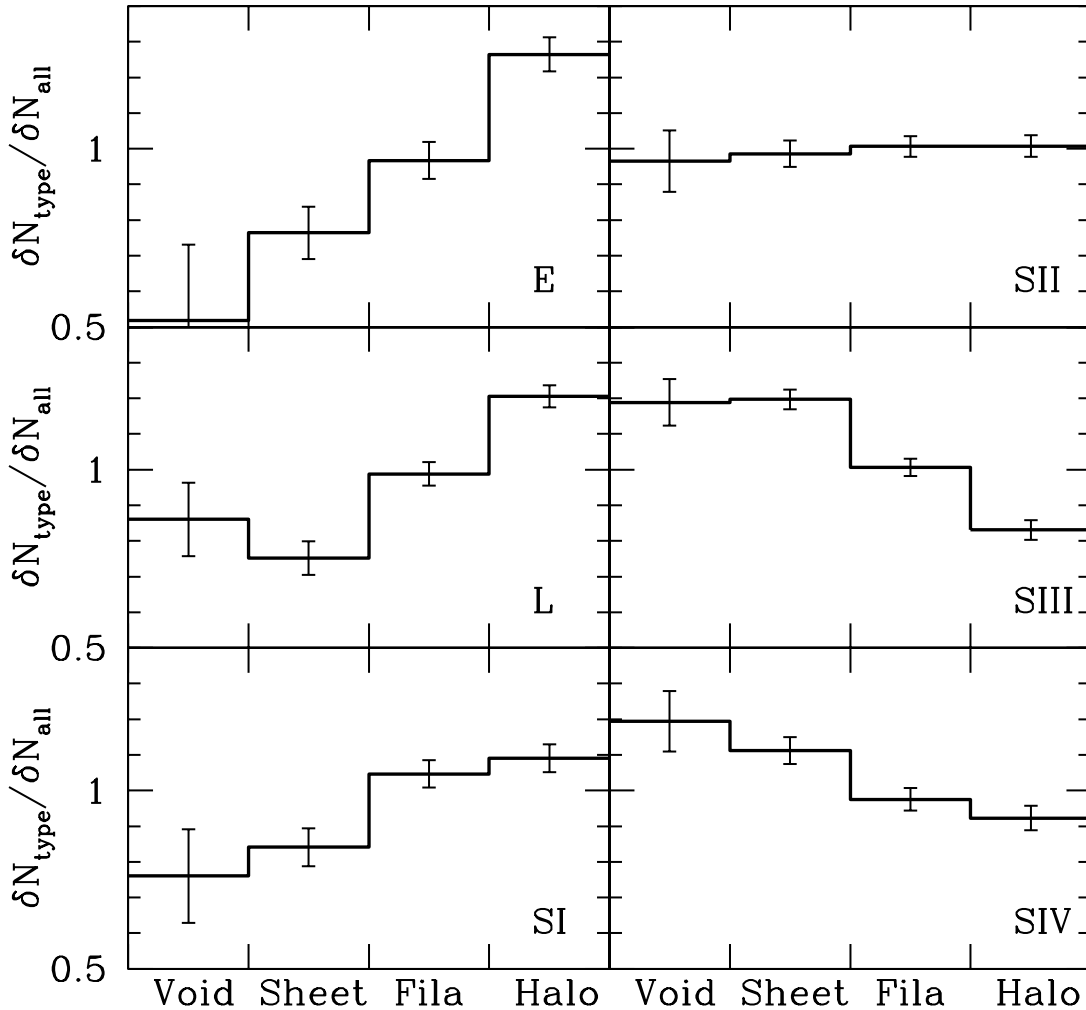


FIG. 3.—Conditional number densities of the galaxies located in voidlike, sheetlike, filament-like, and halo-like regions for the six samples, with Poisson errors.

Here  $N_{\text{type}}$  is the number of galaxies belonging to a given sample,  $\Delta N_{\text{type}}$  is the number of those galaxies in the sample that are located in halo-like regions,  $N_{\text{all}}$  is the number of all selected Tully galaxies, and  $\Delta N_{\text{all}}$  is the number of those Tully galaxies that are located in halo-like regions. If  $\text{CND} > 1$ , then the galaxies in a given sample have a stronger tendency to be located in halo-like regions than the parent sample.

The CNDs of the galaxies located in voidlike, sheetlike, and filament-like regions are calculated in a similar manner. Figure 3 plots the CNDs as histograms for the six samples, with Poisson errors. As can be seen, all six histograms show distinct behavior: the CND of sample E is highest in halo-like regions and lowest in voidlike regions; the CND of sample L is lowest in sheetlike regions; the CND of sample SI is highest in filament-like regions; the CND of sample SII is almost uniform; the CND of sample SIII is highest in voidlike and sheetlike regions; and the CND of sample SIV is highest in voidlike regions. It is interesting to see that in voidlike regions the CND of the lenticular galaxies has a relatively high value compared with that of the elliptical galaxies.

Although the result in Figure 3 shows clearly that galaxy morphology is correlated with the shear of the surrounding large-scale structure, this should not be directly translated into observational evidence for the existence of an *independent* relationship between galaxy morphology and large-scale shear. Since the signs of the three eigenvalues of the tidal shear are correlated with the local

density, the observed signals shown in Figure 3 could be a result of the well-known correlations between the local density and galaxy morphology. For instance, the observed tendency that elliptical galaxies are more abundant in halo-like regions may be due to the fact that the local density is usually higher in these regions, since the three eigenvalues are all positive and the elliptical galaxies are preferentially located in high-density regions. Therefore, to detect the true relationship between galaxy morphology and the shear of the large-scale structure, one has to use controlled subsamples in which the correlations between galaxy morphology and density are removed. In the following subsection, we pursue this task.

### 3.2. Variation with Ellipticity

The environmental shear at a given galaxy position  $\mathbf{x}$  is caused by the anisotropy in the distribution of the surrounding large-scale structure, which in turn induces an asphericity in the gravitational potential  $\Phi(\mathbf{x})$ . The asphericity of  $\Phi(\mathbf{x})$  can be quantified in terms of ellipticity,  $e$ , defined as

$$e \equiv \frac{\lambda_1 - \lambda_3}{2|\delta|} \quad (2)$$

(Bardeen et al. 1986). Here the sum of the three eigenvalues of the tidal shear equals the dimensionless overdensity,  $\delta \equiv (\rho - \bar{\rho})/\bar{\rho}$ , where  $\bar{\rho}$  is the background density:  $\delta = \sum_{i=1}^3 \lambda_i$ . If the three

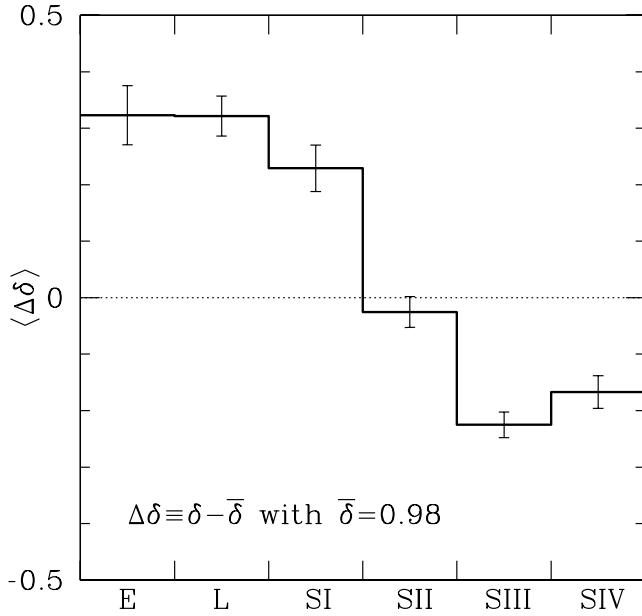


FIG. 4.—Mean of the density difference averaged over the regions where the Tully galaxies of each sample are located. The Tully galaxies are classified into six samples according to morphological type. The errors represent one standard deviation in the measurement of the mean values.

eigenvalues,  $\lambda_1$ ,  $\lambda_2$ , and  $\lambda_3$ , at  $\mathbf{x}$  have the same value, the isopotential surface at  $\mathbf{x}$  has a spherical shape with  $e = 0$ . The larger the differences between  $\lambda_1$  and  $\lambda_3$  are, the higher the value of  $e$  is. If the spatial distribution of galaxies located in a region is highly anisotropic, then the value of  $e$  of the region will be high—in other words, the region has a high ellipticity. The higher the degree of anisotropy in the spatial distribution of the galaxies in a region, the higher the ellipticity the region has.

At the position of each Tully galaxy, we determine the values of  $\delta$  and  $e$ . We first calculate the means of  $\Delta \delta \equiv \delta - \bar{\delta}_G$  averaged separately over each sample listed in Table 1, where  $\bar{\delta}_G$  is the global mean value of the dimensionless overdensity averaged over all selected Tully galaxies. If  $\Delta \delta > 0$ , there is a tendency of the sample galaxies to be located in high-density regions. If  $\Delta \delta < 0$ , the sample galaxies tend to be located in low-density regions. If  $\Delta \delta = 0$  for all six samples, there is no correlation between galaxy morphology and large-scale density. Figure 4 plots  $\langle \Delta \delta \rangle$  for the six samples. As can be seen, there is indeed a strong dependence of galaxy morphology on the large-scale density, which is consistent with the numerical results (Gao et al. 2005).

Next we calculate the means of  $\Delta e \equiv e - \bar{e}_G$  averaged separately over each sample, under the constraint that the value of  $\delta$  is fixed in some narrow range to remove the effect of morphology-density correlations. Note that  $\bar{e}_G$  is averaged in the same constrained range of  $\delta$ . If  $\Delta e > 0$ , there is an *independent* tendency of the sample galaxies to be located in high-shear regions. If  $\Delta e < 0$ , the sample galaxies tend to be located in low-shear regions. If  $\Delta e = 0$  for all six subsamples, there is no correlation between galaxy morphology and large-scale shear.

In the top panel of Figure 5, we plot  $\langle \Delta e \rangle$  for the six samples for the case in which the value of  $\delta$  is fixed in the range  $[-0.3, -0.1]$ . The errors  $\sigma$  are calculated as one standard deviation in the measurement of the mean value:  $\sigma \equiv ([\langle (\Delta e)^2 \rangle] - \langle \Delta e \rangle^2) / (N_g - 1)^{1/2}$ , where  $N_g$  is the number of sample galaxies selected in the given density range. To demonstrate that the correlation between morphology and density is effectively removed by con-

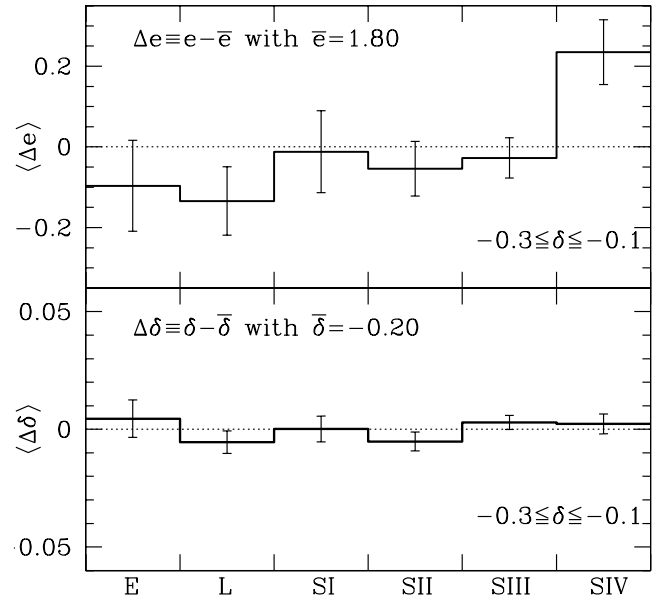


FIG. 5.—Mean of the ellipticity difference (top) and the density difference (bottom) averaged over each subsample with  $\delta$  in the range  $[-0.3, -0.1]$ .

straining the value of  $\delta$  to this range, we also plot  $\langle \Delta \delta \rangle$  for the six subsamples in the bottom panel. As can be seen, the value of  $\langle \Delta \delta \rangle$  is almost uniform, indicating that the morphology-density correlations are controlled to a negligible level with the constraint  $-0.3 \leq \delta \leq -0.1$ . We detect a  $2.9 \sigma$  signal that the mean ellipticity of sample SIV deviates from the global mean ellipticity. This result suggests that the latest-type spirals tend to be located in regions of high ellipticity.

Figure 6 is the same as Figure 5 but with the different constraint  $0.05 \leq \delta \leq 0.1$ . A  $3 \sigma$  signal of morphology-shear correlation is also detected for the sample SIV galaxies. This is consistent with the previous result that the latest-type spirals tend to be preferentially located in high-shear environments. Figure 7 is again the

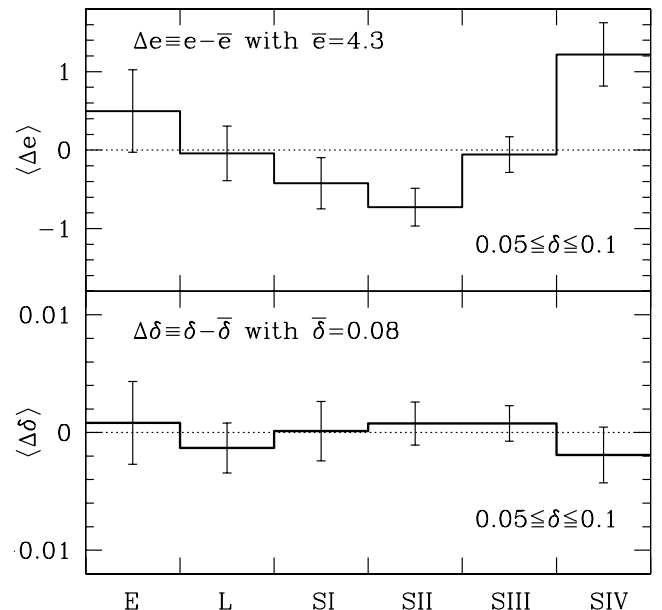
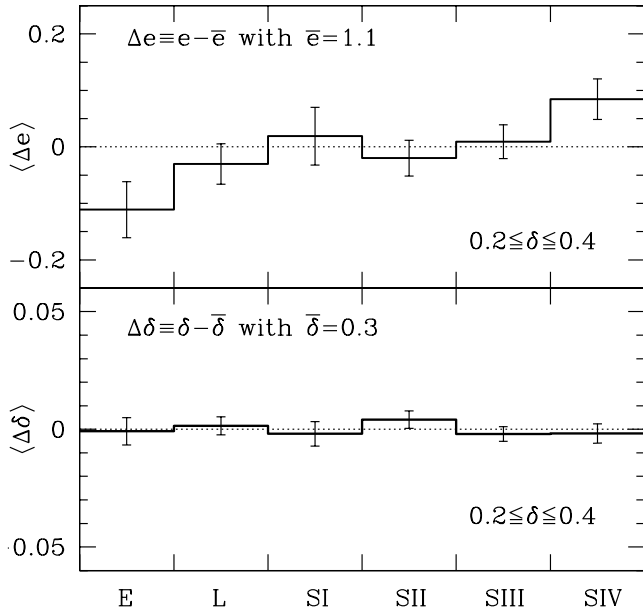
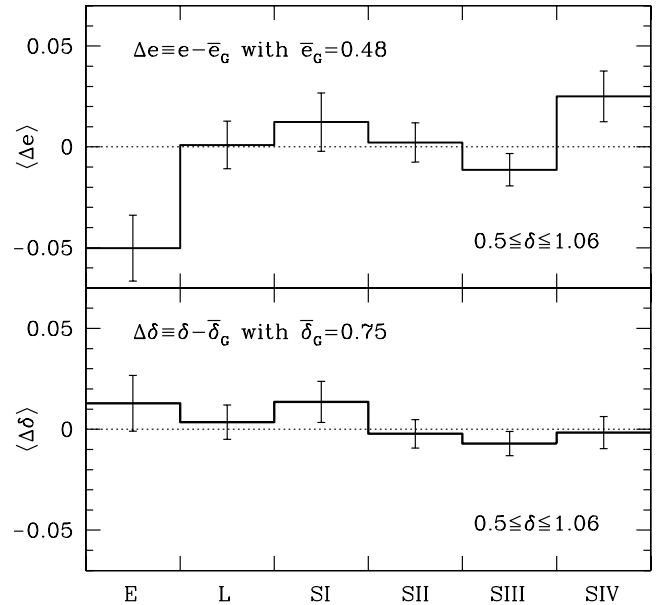


FIG. 6.—Same as Fig. 5, but for  $\delta$  in the range  $[0.05, 0.1]$ .

FIG. 7.— Same as Fig. 5, but for  $\delta$  in the range  $[0.2, 0.4]$ .FIG. 8.— Same as Fig. 5, but for  $\delta$  in the range  $[0.5, 1.06]$ .

same, but with  $\delta$  in the range  $[0.2, 0.4]$ . We detect a  $2.2 \sigma$  signal that the mean ellipticity of the regions where the galaxies of sample E are located is lower than the global mean ellipticity, and a  $2.4 \sigma$  signal that the mean ellipticity of the regions where the galaxies of sample SIV is located is higher than the global mean ellipticity. Figure 8 plots the same but with  $\delta$  in the range  $[0.5, 1.06]$ . There are detected a  $3.1 \sigma$  signal that the mean ellipticity of the regions where the sample E galaxies are located is lower than the global mean ellipticity and a  $2 \sigma$  signal of correlation between the latest-type spirals (SIV) and high-shear regions. The results shown in Figures 7 and 8 indicate consistently that elliptical galaxies tend to be preferentially located in low-shear environments while the latest-type spirals tend to be located in high-shear environments.

Nevertheless, it has to be noted that the galaxy-shear correlation signal is found to be statistically significant only in the bins containing sample E and SIV galaxies. Therefore, when the results over all six bins are considered, the null hypothesis of no galaxy-shear correlation is still quite acceptable. In the given density range, the null hypothesis is found to be rejected at only the  $\sim 10\%$  confidence level when the results over all six bins are considered. Since we consider only galaxies at similar densities, the sample size,  $N_g$ , is quite small, resulting in large statistical errors. It is also worth mentioning that neither in the highly underdense regions with  $\delta < -0.5$  nor in the highly overdense regions with  $\delta > 1.0$  is any signal of galaxy-shear correlation found, since the degree of density-shear correlation is too high to be removed in these regions.

#### 4. DISCUSSION AND CONCLUSIONS

By measuring observationally the mean ellipticities of large-scale structures in which nearby galaxies are embedded as a function of galaxy morphological type, we have tentatively detected an independent relationship between galaxy morphology and environmental shear: In mildly overdense environments, with large-scale dimensionless overdensity  $0.05 \leq \delta \leq 1.06$ , elliptical galaxies are found to prefer low-shear regions; in mildly underdense environments, with large-scale density  $-0.3 \leq \delta \leq -0.1$ , the latest-type spirals (Scd–Sm) are found to prefer high-

shear regions. No correlation signal, however, is found either in the highly overdense ( $\delta > 1$ ) or in the highly underdense ( $\delta < -0.5$ ) environments.

This observational result may be explained by the dependence of halo formation epoch on the shear of the large-scale environment. It is known that the formation epochs of galactic halos depend not only on mass but also on the density of the large-scale environment (Gao et al. 2005). Here we argue that there is some observational evidence to support the hypothesis that the formation epochs of halos also depend on the shear of the large-scale environment. In high-shear environments, the halos form relatively early without growing at late times, as a result of strong tidal disruption from the surrounding matter distribution. Thus, late-type spirals are likely to be located in such high-shear environments. Meanwhile, in low-shear environments the halos formed relatively recently, since there is no strong tidal distribution, having grown at late times through hierarchical merging. Hence, the elliptical galaxies are likely to be found in such low-shear environments. In highly overdense regions, however, even in the case that there is tidal disruption from the surrounding matter distribution, the other, stronger environmental processes should mask the shear dependence of galaxy properties. Likewise, in highly underdense regions the tidal field is too weak to produce any significant galaxy-shear correlation. It will be interesting to test against  $N$ -body simulations whether the formation epoch of galactic halos with similar mass at similar density is a function of the ellipticity of the large-scale dark matter distribution. Our future work is aimed in this direction.

It should be noted here that our results suffer from low statistical significance due to the small sample size. We have seen only a marginal effect of large-scale shear for the latest-type spirals (Scd–Sm). Meanwhile, no signal was found for Sb–Sc galaxies even though both types occupy similar regions. To remove the effect of the stronger galaxy-density correlations, we had to constrain the overdensities of galactic regions, which results in large errors. The null hypothesis that there is no galaxy-shear correlation over the six bins is rejected at only the 10% level because of the large errors. Given our result, a sample of more than 100,000 galaxies will be required in order to test the hypothesis at better than 90% confidence. This line of investigation will provide new insight

into the formation and evolution of galaxies in the filamentary cosmic web.

We are very grateful to P. Erdoğdu for providing us the 2MRS density field. We also thank an anonymous referee who helped us improve significantly the original manuscript by making many helpful suggestions. This work is supported by a Korea Science and Engineering Foundation grant funded by the Korean Ministry of Science and Technology (No. R01-2007-000-10246-0). The

2MRS density field was constructed by Erdoğdu et al. (2006) by making use of data products from the Two Micron All Sky Survey, which is a joint project of the University of Massachusetts and the Infrared Processing and Analysis Center/California Institute of Technology, funded by the National Aeronautics and Space Administration and the National Science Foundation, and the NASA/IPAC Extragalactic Database, which is operated by the Jet Propulsion Laboratory, California Institute of Technology, under contract with the National Aeronautics and Space Administration, and the SIMBAD database, operated at CDS, Strasbourg, France.

#### REFERENCES

- Bardeen, J. M., Bond, J. R., Kaiser, N., & Szalay, A. S. 1986, *ApJ*, 304, 15
- Bernardi, M., Nichol, R. C., Sheth, R. K., Miller, C. J., & Brinkmann, J. 2006, *AJ*, 131, 1288
- Blanton, M. R., Eisenstein, D., Hogg, D. W., Schlegel, D. J., & Brinkmann, J. 2005, *ApJ*, 629, 143
- Bond, J. R., Kofman, L., & Pogosyan, D. 1996, *Nature*, 380, 603
- Cervantes-Sodi, B., & Hernandez, X. 2008, *Rev. Mex. AA*, in press (arXiv:0802.3689)
- Choi, Y.-Y., Park, C., & Vogeley, M. S. 2007, *ApJ*, 658, 884
- Croton, D. J., Gao, L., & White, S. D. M. 2007, *MNRAS*, 374, 1303
- de Vaucouleurs, G., de Vaucouleurs, A., Corwin, H. G., Jr., Buta, R. J., Paturel, G., & Fouqué, P. 1991, *Third Reference Catalogue of Bright Galaxies* (New York: Springer)
- Dressler, A. 1980, *ApJ*, 236, 351
- Erdoğdu, P., et al. 2006, *MNRAS*, 373, 45
- Gao, L., Springel, V., & White, S. D. M. 2005, *MNRAS*, 363, L66
- Gómez, P. L., et al. 2003, *ApJ*, 584, 210
- Goto, T., Yamauchi, C., Fujita, Y., Okamura, S., Sekiguchi, M., Smail, I., Bernardi, M., & Gómez, P. L. 2003, *MNRAS*, 346, 601
- Hernandez, X., & Cervantes-Sodi, B. 2006, *MNRAS*, 368, 351
- Hernandez, X., Park, C., Cervantes-Sodi, B., & Choi, Y.-Y. 2007, *MNRAS*, 375, 163
- Hockney, R. W., & Eastwood, J. W. 1988, *Computer Simulation Using Particles* (New York: Taylor & Francis)
- Kaiser, N. 1984, *ApJ*, 284, L9
- Kuehn, F., & Ryden, B. S. 2005, *ApJ*, 634, 1032
- Lauberts, A. 1982, *The ESO/Uppsala Survey of the ESO (B) Atlas* (Garching: ESO)
- Lee, J., & Erdoğdu, P. 2007, *ApJ*, 671, 1248
- Lewis, I., et al. 2002, *MNRAS*, 334, 673
- Navarro, J. F., Abadi, M. G., & Steinmetz, M. 2004, *ApJ*, 613, L41
- Nilson, P. 1973, *Uppsala Astron. Obs. Ann.*, 6, No. 1
- Pandey, B., & Bharadwaj, S. 2006, *MNRAS*, 372, 827
- . 2008, *MNRAS*, 387, 767
- Park, C., Choi, Y.-Y., Vogeley, M. S., Gott, J. R., III, & Blanton, M. R. 2007, *ApJ*, 658, 898
- Postman, M., & Geller, M. J. 1984, *ApJ*, 281, 95
- Rojas, R. R., Vogeley, M. S., Hoyle, F., & Brinkmann, J. 2005, *ApJ*, 624, 571
- Springel, V., et al. 2005, *Nature*, 435, 629
- Trujillo, I., Carretero, C., & Patiri, S. G. 2006, *ApJ*, 640, L111
- Whitmore, B. C., Gilmore, D. M., & Jones, C. 1993, *ApJ*, 407, 489